·Letter·
Advances in Polar Science
doi: 10.13679/j.advps.2020.0026
December 2020 Vol. 31 No. 4: 291-298

Large spread across AeroCom Phase II models in simulating black carbon in melting snow over Arctic sea ice

PAN Shifeng[1,2,3] & DUAN Mingkeng[1,2,3*]

[1] Collaborative Innovation Center on Forecast and Evaluation of Meteorological Disasters (CIC-FEMD), Nanjing University of Information Science & Technology, Nanjing 210044, China;
[2] Key Laboratory of Meteorological Disaster, Ministry of Education (KLME), Nanjing University of Information Science & Technology, Nanjing 210044, China;
[3] Joint International Research Laboratory of Climate and Environment Change (ILCEC), Nanjing University of Information Science & Technology, Nanjing 210044, China

Received 10 August 2020; accepted 11 November 2020; published online 16 December 2020

Abstract Over two dozen global atmospheric chemistry models contributing to the Aerosol Comparisons between Observations and Models (AeroCom) project were used in this study to drive the Los Alamos sea ice model to simulate the black carbon (BC) concentration in melting snow on Arctic sea ice. Measurements of BC during the melting season show concentrations in the range 2.8–41.6 ng·g^{-1} (average: 15.3 ng·g^{-1}) in the central Arctic Ocean and Canada Basin. Most results from models contributing to the Phase I project were within the 25th and 75th percentiles of the observations, and the multimodel mean was slightly lower than that of the observations. In contrast, there was larger divergence among the Phase II model simulations and the mean value of BC was overestimated. The multimodel mean bias was −3.1 (−11.2 to +6.7) ng·g^{-1} for Phase I models and +3.9 (−9.5 to +21.3) ng·g^{-1} for Phase II models. The differences between the models of the two phases were probably attributable to the updated aerosol scheme in the new contributions, in which removal processes are parameterized by considering the actual dimensions and chemical compositions of the particles. This means the removal mechanism acts in a way that is more selective and leads to more BC particles being transported to the Arctic. In addition, higher spatial resolution could be another important reason for overestimation of BC concentration in snow in Phase II models.

Keywords **black carbon, AeroCom, melting snow, Arctic sea ice**

Citation: Pan S F, Duan M K. Large spread across AeroCom Phase II models in simulating black carbon in melting snow over Arctic sea ice. Adv Polar Sci, 2020, 31(4): 291-298, doi: 10.13679/j.advps.2020.0026

1 Introduction

Black carbon (BC) is among the particulate species most efficient at absorbing visible light (Bond et al., 2013). BC that originates from mid–high-latitude anthropogenic emissions can reach the Arctic and influence the local climate through direct radiative forcing, semidirect cloud effects, indirect cloud effects, and deposition onto snow and ice surfaces (Quinn et al., 2011). In the Arctic, BC deposition can effectively reduce the surface albedo, leading to more rapid ablation of snowpack and its underlying sea ice (Hansen et al., 2004; Flanner et al., 2007; McConnell et al., 2007; Holland et al., 2012; Goldenson et al., 2012). Previous related studies suggested that the annual mean radiative forcing over the Arctic region attributable to BC deposition is 0.1–0.3 W·m^{-2} (Flanner et al., 2009;

*Corresponding author, E-mail: mingkeng@nuist.edu.cn

Quinn et al., 2011; Zhou et al., 2012; Jiao et al., 2014). However, considerable uncertainty remains regarding this effect in the sea ice region owing to lack of field measurements and model verification.

Many measurements of BC concentration in snow have been conducted in the Arctic during various seasons (e.g., Grenfell et al., 2002; Forsström et al., 2009; Doherty et al., 2010; Sinha et al., 2017, 2018; Jacobi et al., 2019). Previous studies have provided extensive verification of modeled BC deposition using ground observations during spring (e.g., Flanner et al., 2007; Wang et al., 2011; Dou et al., 2012; Jiao et al., 2014). In contrast, simulations of BC deposition and of its effect on snow and ice ablation in the melting season are poorly validated and thus considerable uncertainties remain (Dou et al., 2016), especially over the Arctic Ocean. It is well known that BC particles could accumulate at the surface layer of the snowpack through melting of snow, strengthening BC–snow albedo feedbacks (Doherty et al., 2013; Dou et al., 2017; Dou et al., 2019). Therefore, uncertainties regarding BC deposition and the redistribution of BC particles in melting snow might be amplified in modeling of sea ice ablation.

It is necessary to validate the modeled results of BC in melting snow to reduce the uncertainty of such simulations over sea ice areas in the melting season. The Aerosol Comparisons between Observations and Models (AeroCom) project was initiated to allow the aerosol observation and modeling communities to enhance understanding of global aerosols and of their impact on climate (Samset et al., 2013). A large number of atmospheric chemistry and climate models have contributed to the AeroCom archive (Koch et al., 2009; Myhre et al., 2013). Here, we assessed the performance of state-of-the-art aerosol models in simulating BC in melting snow over Arctic sea ice using observations published in earlier studies (Perovich et al., 2009; Doherty et al., 2010; Dou et al., 2012). Two phases of AeroCom models were considered in this study, and the differences between the two sets of modeled results and the intermodel divergences were analyzed.

2 Data and methods

Monthly gridded fields of BC deposition output from 12 (13) models contributing to Phase I (II) of the AeroCom project were used to simulate the BC concentration in melting snow over Arctic sea ice. Table 1 summarizes the names,

Table 1 Phase I and Phase II AeroCom models used in this study

Phase	Model	Resolution (lon×lat×lev)	Global emission rate/(Tg·a^{-1})	Aerosol scheme	References
I	DLR	96°×48°×19	7.77		Ackermann et al.,1998
I	GISS	72°×46°×20	7.77		Koch et al., 2006
I	LOA	96°×73°×19	7.77		Reddy et al., 2004
I	LSCE	96°×73°×19	7.77		Szopa et al., 2013
I	MATCH	192°×94°×28	7.77		Barth et al., 2000
I	MPI-HAM	192°×96°×31	7.77		Stier et al., 2005
I	TM5	60°×45°×25	7.77		Krol et al., 2005
I	UIO-CTM	128°×64°×40	7.77		Grini et al., 2005
I	UIO-GCM	128°×64°×18	7.77		Iversen et al., 2002
I	UIO-GCM-V2	128°×64°×26	7.77		Seland et al., 2008
I	ULAQ	16°×19°×26	7.77		Pitari et al., 2008
I	UMI	144°×91°×30	7.77		Liu et al., 2002
II	CAM4-Oslo	144°×96°×26	10.62		Kirkevåg et al., 2013
II	CAM5.1	144°×96°×30	7.76	Microphysics	Liu et al., 2012
II	ECHAM5-HAM2	192°×96°×31	8.11	Microphysics	Zhang et al., 2012
II	GISS-MATRIX	144°×90°×40	7.58	Microphysics	Bauer et al., 2010
II	GISS-modelE	144°×90°×40	7.59	Bulk	Koch et al., 2007
II	GLOMAP	128°×64°×31	8.13	Microphysics	Spracklen et al., 2011
II	GMI	144°×91°×42	7.76		Bian et al., 2009
II	HadGEM2	192°×145°×38	6.63		Bellouin et al., 2011
II	OsloCTM2	128°×64°×60	7.8	M7 aerosol microphysical module	Myhre et al., 2009
II	SPRINTARS	320°×160°×56	8.12	Microphysics	Takemura et al., 2009
II	TM5	120°×90°×34	8.22	Microphysics	Vignati et al., 2010
II	IMPACT	144°×91°×30	10.55	Microphysics	Yun et al., 2012
II	GOCART	144°×91°×30	10.34		Chin et al., 2009

resolutions, and emission rates of the 25 models. Phase I simulations were performed under the present-day "B" protocol (Kinne et al., 2006) with all models adopting harmonized BC emissions fields, while Phase II simulations were performed under the present-day "A2 control" protocol (Schulz et al., 2009) with each model adopting its own emissions fields.

All fields of BC deposition were regridded to 1.9° × 2.5° resolution and used to drive the Los Alamos sea ice (CICE) model with NCEP/NCAR reanalysis data (with 6-h temporal resolution) in 2005, 2008, and 2010, which is when the BC measurements were conducted. This model is able to simulate the effects of BC deposition, meltwater scavenging, and sublimation on the vertical profile of BC within snow cover. Further details regarding the performance of the CICE model can be found in Holland et al. (2012). For hydrophilic and hydrophobic BC, the scavenging coefficients were set at 0.2 and 0.03, respectively, according to Flanner et al. (2007) and Jiao et al. (2014).

The CICE model includes two snow layers on the sea ice surface, and the thickness of the surface snow varied with the modeled depth of the entire snow layer (Hunke et al., 2011). For example, for thick snow (>8 cm), the surface snow layer was specified as 4 cm, while for thin snow (≤8 cm), the surface snow layer was set at half the total thickness (Holland et al., 2012). On average, during the sampling period, the observed snow depth was approximately 5 cm (Dou et al., 2013). Thus, we used the snow water equivalent of the different layers as weights when calculating the weighted average of the BC concentration in the entire snow layer, which we then compared with the observations obtained during the same period. The spatial distribution of the observations used for model verification is shown in Figure 1 and further details are listed in Table S1. As snow melts, superimposed ice will form on the sea ice surface, some of which will mix with the depth hoar at the bottom of the snow layer (Dou et al., 2012). In practice, it is difficult to distinguish between them during the sampling process. Therefore, BC concentrations in "snow/ice samples" were used to validate the model results in this study. For measurement sites within the same model grid, the observed values were averaged to provide a single value for comparison with the modeled value.

3 Results and discussion

Based on the observations on BC in snow on Arctic sea ice, collated from earlier studies (Table S1), we estimated that the BC concentration in melting snow over the central Arctic Ocean and Canada Basin was in the range 2.8–41.6 ng·g^{-1} (average: 15.3 ng·g^{-1}). Before verification, the model results were interpolated to each measurement site in the corresponding month and year of the observations and compared with the mean observed value in cases where

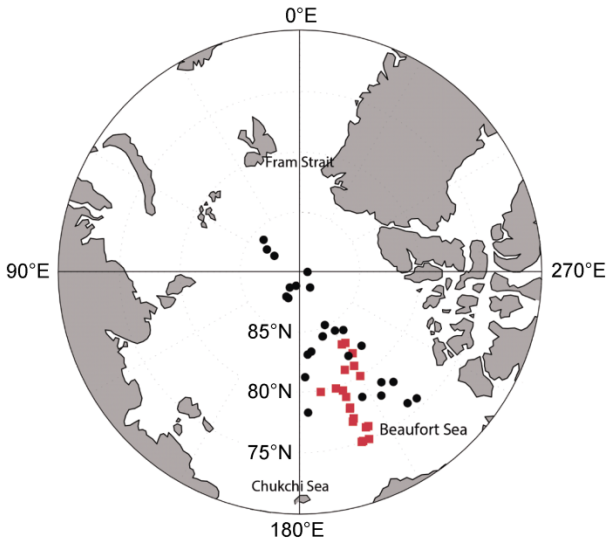

Figure 1 Distribution of measurement sites used in this study. Red squares indicate measurement sites during the 1st Korean Arctic Expedition in summer 2010 (Dou et al., 2012). Black circles indicate the observations provided by Doherty et al. (2010), involving measurements conducted during the HOTRAX* campaign in summer 2005 and during the UVic** campaign in summer 2008. During these three campaigns, the melting snow on Arctic sea ice was sampled. Notes: *The Healy-Oden Trans-Arctic Expedition (HOTRAX) was a summer transect of the Arctic Ocean from the Bering Strait to Fram Strait performed by two icebreakers (*Oden* and *Healy*) in 2005. **The UVic campaign was a summer transect in the Beaufort Sea coordinated by the University of Victoria in 2008.

more than one measurement was available within a model grid box. Observation–model comparison revealed that all the model results were within the observed minimum and maximum thresholds, although intermodel divergence was large. In comparison with the mean value of the observations, the multimodel mean bias was −3.1 (−11.2 to +6.7) ng·g^{-1} for Phase I models and +3.9 (−9.5 to +21.3) ng·g^{-1} for Phase II models. The results of most Phase I models were concentrated within the 25th and 75th percentiles of the observations, and the average value of the multimodel results was slightly lower than that of the observations (Figure 2). In contrast, model divergence was more apparent in the Phase II contributions, and the mean value of BC concentration was overestimated (Figure 2). Overestimation of the multimodel mean for the Phase II models was mainly driven by overestimation in OsloCTM2, HadGEM2, GOCART, and TM5.

In this study, all simulations were conducted using the same sea ice model driven by the same atmospheric reanalysis data and different atmospheric chemistry models. Thus, the simulated discrepancies of BC values in melting snow were attributable mainly to intermodel diversity in BC deposition. The simulation of BC deposition depends on the emission inventory, parameterizations of aerosol aging,

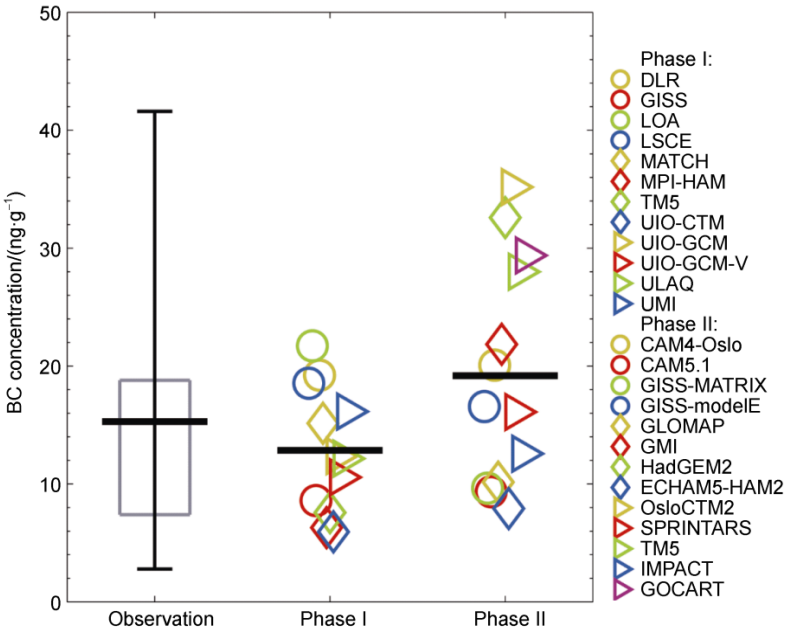

Figure 2 Observed and modeled BC values within melting snow over Arctic sea ice. From left to right: observed snow BC, simulated concentrations over the observational domain based on AeroCom Phase I models, and simulated values from Phase II models. The gray box indicates the 25th and 75th percentiles of the observations, and the whiskers depict the threshold of observed minimum and maximum values. The bold horizontal line indicates the mean value of the observations/multimodel results. Each colored dot represents the mean result of a particular model averaged over the grid cells matching the location, time, and depth of the measurements.

aerosol–cloud interactions, and dry and wet removal processes (Quinn et al., 2011). In this study, Phase I models adopted harmonized BC emissions fields (Table 1), although possibly with slight differences in the partitioning of emissions in terms of the vertical space and size distributions. In contrast, each Phase II model adopted its own emissions, for which the emission rates had a normalized standard deviation of 0.23 (Table 1), leading to wider divergence in model deposition flux. Therefore, part of the increased spread in Phase II BC concentrations in snow originated from the use of different emissions inventories.

The most important update in the Phase II contributions is the incorporation of a new aerosol scheme. Phase I models apply an aerosol process described as a bulk scheme (Krol et al., 2005). For bulk models, wet removal is overestimated because BC particles are considered wholly soluble in clouds, and because the hygroscopic state and particle size are not taken into account. In contrast, for most models contributing to Phase II (e.g., TM5, OsloCTM2, HadGEM2, GOCART, SPRINTARS, GMI, and GISS), a new version of aerosol dynamics is applied (Gilardoni et al., 2011; Mann et al., 2014). In these models, aerosol particles are described in modes with coagulation, condensation, and nucleation considered. The removal processes are parameterized by considering the actual dimensions and chemical compositions of the particles (Glassmeier et al., 2017). Therefore, the new aerosol scheme allows the removal mechanism of BC aerosols to act in a way that is more selective and physically realistic, leading to transportation of BC particles to the Arctic that is more effective (Sand et al., 2017). This is the main reason for the overestimation of BC in melting snow and for the more significant intermodel divergence in Phase II models. In addition, it can be seen that most Phase II models run with higher horizontal resolution (Table 1). Previous studies have indicated that underestimation of aerosol concentrations in the Arctic could be improved in part by increasing the horizontal resolution of the models (e.g., Wiedinmyer et al., 2011; Ma et al., 2014), which might be an important reason for the overestimation of BC concentrations in snow in Phase II models.

Comparison of the model results and observations in the domain of the field measurements revealed that snow depth was overestimated by approximately 3.5 cm on average during the measurement period, leading to overestimation of the total snow BC content in the snow layer. This was expected because the CICE model does not consider the impact of snow drift (Hunke et al., 2011; Blanchard-Wrigglesworth et al., 2015). Affected by impurity enrichment associated with melting snow in the model, the snow BC concentration will be overestimated. This is another reason for the overestimation in Phase II models.

Comparison of the results of each model in terms of the average, maximum, and minimum values and spatial variability (correlation coefficient) revealed that among the

Phase I models, MATCH and UMI could well reproduce the observed value of BC over the measurement area, and that the average value of each model was within the 25th and 75th percentiles of the observations (Table 2). For Phase II models, the results of GISS-modelE were most comparable with the observations (Table 3).

Table 2 Comparison of the results from Phase I models and the observations

	Observation	DLR	GISS	LOA	LSCE	MATCH	MPI-HAM	TM5	UIO-CTM	UIO-GCM	UIO-GCM-V2	ULAQ	UMI
Maximum	41.6	72.2	25.3	76.41	55.77	53.21	16.65	21.67	22.53	36.75	25.31	33.7	59.1
Minimum	2.8	1.94	0.91	1.86	1.63	1.56	0.58	1.24	0.78	1.54	1.52	2.55	1.7
Average	15.3	19.23	8.59	21.73	18.55	15.15	6.29	7.58	5.95	12.37	10.55	12.15	16.14
Obs & Mod: r	——	0.25	0.26	0.29	**0.32***	**0.34***	0.29	0.25	0.20	**0.31***	0.18	0.21	**0.36***

Note: ∗denotes $P<0.05$.

Table 3 Comparison of the results from Phase II models and observations

	Observation	CAM5.1	CAM4-Oslo	ECHAM5-HAM2	GISS-MATRIX	GISS-modelE	GLOMAP	GMI	GOCART	HadGEM2	IMPACT	OsloCTM2	SPRINTARS	TM5
Maximum	41.6	17.06	57.6	31.7	24.22	53.92	27.17	66.76	94.83	91.52	23.17	126.48	53.49	83
Minimum	2.8	1.73	2.53	1.36	2.22	3.32	1.65	2.89	4.61	6.99	2.41	4.99	1.84	3.86
Average	15.3	9.33	20.08	7.92	9.63	16.56	10.15	21.85	29.39	32.58	12.57	35.18	16.11	27.99
Obs & Mod: r	——	0.17	**0.31***	0.21	0.21	0.32*	**0.25**	0.25	0.24	0.26	0.17	0.18	0.21	0.32*

Note: ∗ denotes $P<0.05$.

4 Conclusions

Two dozen state-of-the-art global atmospheric chemistry models contributing to the AeroCom project were used to drive the CICE model to simulate BC concentration in melting snow over Arctic sea ice. Results showed that the multimodel average of the models contributing to Phase I could generally reproduce the mean level of observed BC concentrations over the Arctic Ocean and Canada Basin, and most of the simulated BC values were concentrated within the 25th and 75th percentiles of the observations. The dispersion in the results of the Phase II models was larger and the mean value of the multimodel results was overestimated in comparison with the observed average concentration. The main reason is the adoption of a new and more selective aerosol scheme in the Phase II models that reduces the BC scavenging efficiency and increases intermodel differences. Overall, the Phase II multimodel results showed no significant improvement in the simulation of BC concentration in melting snow, but did indicate increased intermodel discrepancies.

In terms of individual models, the MATCH and UMI (Phase I) and GISS-modelE (Phase II) models showed better performance in simulation of BC concentration in melting snow over Arctic sea ice. To provide reasonable estimations of BC concentration in melting snow and of its radiative forcing effect over Arctic sea ice, it would be beneficial to first select the optimal models through comparison with observed vertical profiles of aerosol BC in the Arctic, and then use the selected models to drive the sea ice model. Of course, more extensive observations of BC concentration in melting snow will be necessary for model verification. Meanwhile, further improvement is needed regarding the parameterization of BC scavenging associated with melting snow because the redistribution and/or enrichment of BC particles can greatly affect the BC concentration in melting snow.

Acknowledgments This study is funded by the Program of National Natural Science Foundation of China (Grant nos. 41675056 and 41991283). We are grateful to the High-Performance Computing Center of Nanjing University of Information Science & Technology for conducting the numerical calculations. The authors thank the reviewer, Dr. H W Jacobi, and another anonymous reviewer for their constructive comments and suggestions.

References

Ackermann I J, Hass H, Memmesheimer M, et al. 1998. Modal aerosol dynamics model for Europe: development and first applications. Atmos Environ, 32(17): 2981-2999, doi: 10.1016/s1352-2310(98)00006-5.

Barth M C, Rasch P J, Kiehl J T, et al. 2000. Sulfur chemistry in the National Center for Atmospheric Research Community Climate Model: Description, evaluation, features, and sensitivity to aqueous chemistry. J Geophys Res, 105(D1): 1387-1415, doi: 10.1029/1999jd900773.

Bauer S E, Menon S, Koch D, et al. 2010. A global modeling study on carbonaceous aerosol microphysical characteristics and radiative effects. Atmos Chem Phys, 10(15): 7439-7456, doi: 10.5194/acp-10-7439-2010.

Bellouin N, Rae J, Jones A, et al. 2011. Aerosol forcing in the Climate

Model Intercomparison Project (CMIP5) simulations by HadGEM2-ES and the role of ammonium nitrate. J Geophys Res, 116(D20): D20206, doi: 10.1029/2011jd016074.

Bian H, Chin M, Rodriguez J M, et al. 2009. Sensitivity of aerosol optical thickness and aerosol direct radiative effect to relative humidity. Atmos Chem Phys, 9(7): 2375-2386, doi: 10.5194/acp-9-2375-2009.

Blanchard-Wrigglesworth E, Farrell S L, Newman T, et al. 2015. Snow cover on Arctic sea ice in observations and an Earth System Model. Geophys Res Lett, 42(23): 10342-10348, doi: 10.1002/2015gl066049.

Bond T C, Doherty S J, Fahey D W, et al. 2013. Bounding the role of black carbon in the climate system: A scientific assessment. J Geophys Res Atmos, 118(11): 5380-5552, doi: 10.1002/jgrd.50171.

Chin M, Diehl T, Dubovik O, et al. 2009. Light absorption by pollution, dust, and biomass burning aerosols: a global model study and evaluation with AERONET measurements. Ann Geophys, 27(9): 3439-3464, doi: 10.5194/angeo-27-3439-2009.

Doherty S J, Grenfell T C, ForsstrÖm S, et al. 2013. Observed vertical redistribution of black carbon and other insoluble light-absorbing particles in melting snow. J Geophys Res Atmos, 118: 5553-5569, doi: 10.1002/jgrd.50235.

Doherty S J, Warren S G, Grenfell T C, et al. 2010. Light-absorbing impurities in Arctic snow. Atmos Chem Phys, 10(8): 11647-11680, doi: 10.5194/acp-10-11647-2010.

Dou T, Du Z, Li S, et al. 2019. Brief communication: An alternative method for estimating the scavenging efficiency of black carbon by meltwater over sea ice. Cryosphere Discuss, 13(12): 3309-3316, doi: 10.5194/tc-2019-147.

Dou T, Xiao C. 2013. Measurements of physical characteristics of summer snow cover on sea ice during the Third Chinese Arctic Expedition. Sci Cold Arid Reg, 5(3): 309-315, doi: 10.3724/SP.J.1226.2013.00309.

Dou T, Xiao C. 2016. An overview of black carbon deposition and its radiative forcing over the Arctic. Adv Clim Chang Res, 7(3): 115-122.

Dou T, Xiao C, Du Z, et al. 2017. Sources, evolution and impacts of EC and OC in snow on sea ice: a measurement study in Barrow, Alaska. Sci Bull, 62(22): 1547-1554, doi:10.1016/j.scib.2017.10.014.

Dou T, Xiao C, Shindell D T, et al. 2012. The distribution of snow black carbon observed in the Arctic and compared to the GISS-PUCCINI model. Atmos Chem Phys, 12(17): 7995-8007, doi: 10.5194/acp-12-7995-2012.

Flanner M G, Zender C S, Hess P G, et al. 2009. Springtime warming and reduced snow cover from carbonaceous particles. Atmos Chem Phys, 9: 2481-2497.

Flanner M G, Zender C S, Randerson J T, et al. 2007. Present-day climate forcing and response from black carbon in snow. J Geophys Res, 112: D11202, doi: 10.1029/2006jd008003.

Forsström S, Strom J, Pedersen C A, et al. 2009. Elemental carbon distribution in Svalbard snow. J Geophys Res, 114: D19112, doi: 10.1029/2008JD011480.

Gilardoni S, Vignati E, Wilson J. 2011. Using measurements for evaluation of black carbon modeling. Atmos Chem Phys, 11: 439-455, doi: 10.5194/acp-11-439-2011.

Glassmeier F, Possner A, Vogel B, et al. 2017. A comparison of two chemistry and aerosol schemes on the regional scale and the resulting impact on radiative properties and liquid and ice-phase aerosol–cloud interactions. Atmos Chem Phys, 17: 8651-8680, doi: 10.5194/acp-17-8651-2017.

Goldenson N, Doherty S J, Bitz C M, et al. 2012. Arctic climate response to forcing from light-absorbing particles in snow and sea ice in CESM. Atmos Chem Phys, 12: 7903-7920, doi: 10.5194/acp-12-7903-2012.

Grenfell T, Light B, Sturm M. 2002. Spatial distribution and radiative effects of soot in the snow and sea ice during the SHEBA experiment. J Geophys Res, 107(C10): SHE 7-1-SHE 7-7, doi: 10.1029/2000JC 000414.

Grini A, Myhre G, Zender C S, et al. 2005. Model simulations of dust sources and transport in the global atmosphere: Effects of soil erodibility and wind speed variability. J Geophys Res, 110(2): 1-14, doi: 10.1029/2004JD005037.

Hansen J, Nazarenko L. 2004. Soot climate forcing via snow and ice albedos. Proc Natl Acad Sci, 101(2): 423-428, doi: 10.1073/pnas. 2237157100.

Holland M, Bailey D A, Briegleb B P, et al. 2012. Improved sea ice shortwave radiation physics in CCSM4: The impact of melt ponds and aerosols on Arctic sea ice. J Clim, 25(5): 1413-1430, doi: 10.1175/ JCLI-D-11-00078.1.

Hunke E C, Lipscomb W H, Turner A K. 2011. Sea-ice models for climate study: retrospective and new directions. J Glaciol, 56(200): 1162-1172.

Iversen T, Seland Ø. 2002. A scheme for process-tagged SO_4 and BC aerosols in NCAR CCM3: Validation and sensitivity to cloud processes. J Geophys Res, 107(D24): AAC 4-1-AAC 4-30, doi: 10.1029/2001JD000885.

Jacobi H-W, Obleitner F, Costa S D, et al. 2019. Deposition of ionic species and black carbon to the Arctic snowpack: combining snow pit observations with modeling. Atmos Chem Phys, 19(15): 10361-10377, doi: 10.5194/acp-19-10361-2019.

Jiao C, Flanner M G, Balkanski Y, et al. 2014. An AeroCom assessment of black carbon in Arctic snow and sea ice. Atmos Chem Phys, 14(5): 2399-2417, doi: 10.5194/acpd-13-26217-2013.

Kinne S, Schulz M, Textor C, et al. 2006. An AeroCom initial assessment – optical properties in aerosol component modules of global models. Atmos Chem Phys, 6: 1815-1834, doi: 10.5194/acp-6-1815-2006.

Kirkevåg A, Iversen T, Seland Ø, et al. 2013. Aerosol–climate interactions in the Norwegian Earth System Model–NorESM1-M. Geosci Model Dev, 6: 207-244, doi: 10.5194/gmd-6-207-2013.

Koch D, Bond T C, Streets D, et al. 2007. Global impacts of aerosols from particular source regions and sectors. J Geophys Res, 112: D02205, doi: 10.1029/2005JD007024.

Koch D, Schmidt G A, Field C, 2006. Sulfur, sea salt and radionuclide aerosols in GISS ModelE. J Geophys Res, 111: D06206, doi: 10.1029/2004JD005550.

Koch D, Schulz M, Kinne S, et al. 2009. Evaluation of black carbon estimations in global aerosol models. Atmos Chem Phys, 9: 9001-9026.

Krol M, Houweling S, Bregman B, et al. 2005. The two-way nested global chemistry-transport zoom model TM5: algorithm and applications. Atmos Chem Phys, 5: 417-432, doi: 10.5194/acp-5-417-2005.

Liu X, Easter R C, Ghan S J, et al. 2012. Toward a minimal representation of aerosols in climate models: description and evaluation in the Community Atmosphere Model CAM5. Geosci Model Dev, 5: 709-739, doi: 10.5194/gmd-5-709-2012.

Liu X, Penner J E. 2002. Effect of Mount Pinatubo H_2SO_4/H_2O aerosol on ice nucleation in the upper troposphere using a global chemistry and

transport model. J Geophys Res Atmos, 107: AAC 2-1-AAC 2-18, doi: 10.1029/2001JD000455.

Ma P L, Rasch P J, Fast J D, et al. 2014. Assessing the CAM5 physics suite in the WRF-Chem model: implementation, resolution sensitivity, and a first evaluation for a regional case study. Geosci Model Dev, 7(3): 755-778. doi: 10.5194/gmd-7-755-2014.

Mann G W, Carslaw K S, Reddington C L, et al. 2014. Intercomparison and evaluation of global aerosol microphysical properties among AeroCom models of a range of complexity. Atmos Chem Phys, 14: 4679-4713, doi: 10.5194/acp-14-4679-2014.

McConnell J R, Edwards R, Kok G L, et al. 2007. 20th-Century industrial black carbon emissions altered Arctic climate forcing. Science, 317: 1381-1384, doi: 10.1126/science.1144856.

Myhre G, Berglen T F, Johnsrud M, et al. 2009. Modelled radiative forcing of the direct aerosol effect with multi-observation evaluation. Atmos Chem Phys, 9: 1365-1392, doi: 10.5194/acp-9-1365-2009.

Myhre G, Samset B H, Schulz M, et al. 2013. Radiative forcing of the direct aerosol effect from AeroCom Phase II simulations. Atmos Chem Phys, 13: 1853-1877, doi: 10.5194/acp-13-1853-2013.

Perovich D K, Grenfell T C, Light B, et al. 2009. Transpolar observations of the morphological properties of Arctic sea ice. J Geophys Res, 114: C00A04, doi: 10.1029/2008JC004892.

Pitari G, Iachetti D, Mancini E, et al. 2008. Radiative forcing from particle emissions by future supersonic aircraft. Atmos Chem Phys, 8(14): 4069-4084, doi: 10.5194/acp-8-4069-2008.

Quinn P K, Stohl A, Arneth A, et al. 2011. The impact of black carbon on Arctic climate. Arctic Monitoring and Assessment Programme (AMAP), Oslo, 72.

Reddy M S, Boucher O A. 2004. A study of the global cycle of carbonaceous aerosols in the LMDZT general circulation model. J Geophys Res Atmos, 109(D14): D14202, doi: 10.1029/2003JD004048.

Samset B H, Myhre G, Schulz M, et al. 2013. Black carbon vertical profiles strongly affect its radiative forcing uncertainty. Atmos Chem Phys, 13(5): 2423-2434, doi: 10.5194/acp-13-2423-2013.

Sand M, Samset B H, Balkanski Y, et al. 2017. Aerosols at the poles: an AeroCom Phase II multi-model evaluation. Atmos Chem Phys, 17(19): 1-35, doi: 10.5194/acp-2016-1120.

Schulz M, Chin M, Kinne S. 2009. The Aerosol Model Comparison Project, AeroCom, Phase II: Clearing Up Diversity, IGAC Newsletter, Issue No 41, May 2019.

Seland Ø, Iversen T, Kirkevåg A, et al. 2008. Aerosol climate interactions in the CAM-Oslo atmospheric GCM and investigation of associated basic shortcomings. Tellus A, 60: 459-491, doi: 10.1111/j.1600-0870.2008.00318.x.

Sinha P R, Kondo Y, Koike M, et al. 2017. Evaluation of ground-based black carbon measurements by filter-based photometers at two Arctic sites. J Geophys Res Atmos, 122(6): 3544-3572, doi: 10.1002/2016jd 025843.

Sinha P R, Kondo Y, Goto-Azuma K, et al. 2018. Seasonal progression of the deposition of black carbon by snowfall at Ny-Ålesund, Spitsbergen. J Geophys Res Atmos, 123(2): 997-1016, doi: 10.1002/2017jd028027.

Spracklen D V, Carslaw K S, Pöschl U, et al. 2011. Global cloud condensation nuclei influenced by carbonaceous combustion aerosol. Atmos Chem Phys, 11(17): 9067-9087, doi: 10.5194/acp-11-9067-2011.

Stier P, Feichter J, Kinne S, et al. 2005. The aerosol-climate model ECHAM5-HAM. Atmos Chem Phys, 5(4): 1125-1156, doi: 10.5194/acp-5-1125-2005.

Szopa S, Balkanski Y, Schulz M, et al. 2013. Aerosol and ozone changes as forcing for climate evolution between 1850 and 2100. Clim Dyn, 40(9-10): 2223-2250, doi: 10.1007/s00382-012-1408-y.

Takemura T, Egashira M, Matsuzawa K, et al. 2009. A simulation of the global distribution and radiative forcing of soil dust aerosols at the Last Glacial Maximum. Atmos Chem Phys, 9(9): 3061-3073, doi: 10.5194/acp-9-3061-2009.

Vignati E, Karl M, Krol M, et al. 2010. Sources of uncertainties in modelling black carbon at the global scale. Atmos Chem Phys, 10(6): 2595-2611, doi: 10.5194/acp-10-2595-2010.

Wang Q, Jacob D J, Fisher J A, et al. 2011. Sources of carbonaceous aerosols and deposited black carbon in the Arctic in winter-spring: implications for radiative forcing. Atmos Chem Phys, 11(23): 12453-12473, doi: 10.5194/acp-11-12453-2011.

Wiedinmyer C, Akagi S K, Yokelson R J, et al. 2011. The Fire Inventory from NCAR (FINN): a high resolution global model to estimate the emissions from open burning. Geosci Model Dev, 4(3): 625-641, doi: 10.5194/gmd-4-625-2011.

Yun Y, Penner J E. 2012. Global model comparison of heterogeneous ice nucleation parameterizations in mixed phase clouds. J Geophys Res Atmos, 117: D07203, doi: 10.1029/2011JD016506.

Zhou C, Penner J E, Flanner M G, et al. 2012. Transport of black carbon to polar regions: Sensitivity and forcing by black carbon. Geophys Res Lett, 39(22): L22804, doi: 10.1029/2012gl053388.

Zhang K, O'Donnell D, Kazil J, et al. 2012. The global aerosol-climate model ECHAM-HAM, version 2: sensitivity to improvements in process representations. Atmos Chem Phys, 12(19): 8911-8949, doi: 10.5194/acp-12-8911-2012.

Appendix

Table S1 BC concentrations observed in the melting snow over summer Arctic sea ice

No.	Measurement region	Lat /(ºN)	Lon /(ºE)	Sample type	BC concentration /(ng·g^{-1})	Measurement period	Reference
1	Arctic Ocean	75.00	200.01	snow/ice	11.4	Jul, 2010	Dou et al., 2012
2	Arctic Ocean	75.00	202.05	snow/ice	2.8	Jul, 2010	Dou et al., 2012
3	Arctic Ocean	75.03	200.52	snow/ice	7.4	Jul, 2010	Dou et al., 2012
4	Arctic Ocean	75.71	222.08	snow/ice	16.0	Aug, 2005	Perovich et al.,2009
5	Arctic Ocean	75.91	219.41	snow/ice	10.2	Aug, 2008	Doherty et al., 2010
6	Arctic Ocean	75.99	203.05	snow/ice	41.6	Jul, 2010	Dou et al., 2012
7	Arctic Ocean	76.00	203.97	snow/ice	10.2	Jul, 2010	Dou et al., 2012
8	Arctic Ocean	76.81	199.48	snow/ice	40.2	Aug, 2010	Dou et al., 2012
9	Arctic Ocean	77.04	200.18	aged snow	22.1	Aug, 2010	Dou et al., 2012
10	Arctic Ocean	77.07	213.04	snow/ice	10.0	Jul, 2008	Doherty et al., 2010
11	Arctic Ocean	77.09	200.13	snow/ice	39.2	Aug, 2010	Dou et al., 2012
12	Arctic Ocean	77.98	200.36	snow/ice	29.8	Aug, 2010	Dou et al., 2012
13	Arctic Ocean	78.00	220.42	snow/ice	15.0	Aug, 2008	Doherty et al., 2010
14	Arctic Ocean	78.29	183.32	snow/ice	12.3	Aug, 2005	Doherty et al., 2010
15	Arctic Ocean	78.39	206.55	snow/ice	21.6	Aug, 2008	Doherty et al., 2010
16	Arctic Ocean	78.06	216.05	snow/ice	26.0	Aug, 2005	Perovich et al., 2009
17	Arctic Ocean	78.92	200.33	snow/ice	17.8	Aug, 2010	Dou et al., 2012
18	Arctic Ocean	79.51	199.98	aged snow	14.0	Aug, 2010	Dou et al., 2012
19	Arctic Ocean	79.99	210.13	snow/ice	28.9	Aug, 2010	Dou et al., 2012
20	Arctic Ocean	80.98	210.00	snow/ice	6.5	Aug, 2010	Dou et al., 2012
21	Arctic Ocean	79.88	333.99	snow/ice	4.8	Aug, 2008	Doherty et al., 2010
22	Arctic Ocean	81.23	182.81	snow/ice	3.5	Aug, 2005	Doherty et al., 2010
23	Arctic Ocean	81.93	210.07	snow/ice	14.1	Aug, 2008	Doherty et al., 2010
24	Arctic Ocean	81.94	213.01	snow/ice	8.5	Aug, 2010	Dou et al., 2012
25	Arctic Ocean	83.03	210.11	aged snow	13.0	Aug, 2010	Dou et al., 2012
26	Arctic Ocean	81.99	219.94	snow/ice	14.4	Aug, 2008	Doherty et al., 2010
27	Arctic Ocean	83.09	185.33	snow/ice	4.3	Aug, 2005	Doherty et al., 2010
28	Arctic Ocean	83.03	188.11	snow/ice	5.2	Aug, 2005	Doherty et al., 2010
29	Arctic Ocean	83.96	216.81	snow/ice	11.8	Aug, 2005	Doherty et al., 2010
30	Arctic Ocean	84.31	210.92	snow/ice	4.6	Aug, 2005	Doherty et al., 2010
31	Arctic Ocean	84.31	199.35	snow/ice	14.4	Aug, 2005	Doherty et al., 2010
32	Arctic Ocean	84.31	199.58	snow/ice	15.7	Aug, 2005	Doherty et al., 2010
33	Arctic Ocean	85.12	205.2	snow/ice	18.8	Sep, 2005	Doherty et al., 2010
34	Arctic Ocean	85.94	48.34	snow/ice	9.6	Sep, 2005	Doherty et al., 2010
35	Arctic Ocean	86.66	55.62	snow/ice	5.0	Sep, 2005	Doherty et al., 2010
36	Arctic Ocean	87.47	57.59	snow/ice	7.1	Sep, 2005	Doherty et al., 2010
37	Arctic Ocean	87.62	155.88	snow/ice	30.0	Sep, 2005	Doherty et al., 2010
38	Arctic Ocean	87.66	150.09	snow/ice	8.0	Aug, 2005	Perovich et al.,2009
39	Arctic Ocean	88.46	146.53	snow/ice	22.4	Sep, 2005	Doherty et al., 2010
40	Arctic Ocean	88.46	213.47	snow/ice	7.0	Aug, 2005	Perovich et al.,2009
41	Arctic Ocean	88.81	164.14	snow/ice	18.2	Sep, 2005	Doherty et al., 2010
42	Arctic Ocean	89.37	270.91	snow/ice	8.4	Sep, 2005	Doherty et al., 2010